frontiers | Frontiers in Earth Science

TYPE Original Research
PUBLISHED 30 August 2024
DOI 10.3389/feart.2024.1428316



OPEN ACCESS

EDITED BY
Amer A. Shehata,
Texas A&M University Corpus Christi,
United States

REVIEWED BY
Mehdi Ostadhassan,
Northeast Petroleum University, China
Mohammad Abdelfattah Sarhan,
Damietta University, Egypt

*CORRESPONDENCE
Lianbo Zeng,
lbzeng@sina.com

RECEIVED 06 May 2024
ACCEPTED 04 July 2024
PUBLISHED 30 August 2024

CITATION
Lu H, Cao S, Dong S, Lyu W and Zeng L (2024), Control of lamination on bedding-parallel fractures in tight sandstone reservoirs: the seventh member of the upper Triassic Yanchang Formation in the Ordos Basin, China.
*Front. Earth Sci.* 12:1428316.
doi: 10.3389/feart.2024.1428316



# Control of lamination on bedding-parallel fractures in tight sandstone reservoirs: the seventh member of the upper Triassic Yanchang Formation in the Ordos Basin, China

Hao Lu[1,2], Song Cao[1,2], Shaoqun Dong[1,3], Wenya Lyu[1,2] and Lianbo Zeng[1,2]*

[1]State Key Laboratory of Petroleum Resources and Prospecting, China University of Petroleum, Beijing, China, [2]College of Geosciences, China University of Petroleum, Beijing, China, [3]College of Science, China University of Petroleum, Beijing, China

Tight sandstone reservoirs have extremely low porosity and permeability. Bedding-parallel fractures (BPFs) contribute prominently to the storage and seepage capability. However, the distribution of BPFs is remarkably heterogeneous, impeding the prediction and modeling of sweet spots. BPFs are controlled fundamentally by laminations, which are widely distributed in lacustrine tight reservoirs and provide most weakness planes. Based on core and thin section data, BPFs of the upper Triassic Chang 7 tight oil reservoir are characterized microscopically. The lamination combination unit, which is defined by distinctive lamination assemblage and relatively stable lamination thickness and space, is utilized as a homogeneous unit to measure the density of lamination and related BPFs. The influence of laminations on BPFs is discussed further. Results show that most bedding-parallel fractures are unfilled, with apertures generally <40 μm, mainly <10 μm. Larger apertures correlate with low filling degrees. The distribution of BPFs is intricately controlled by lamination type, density, and thickness. (1) BPFs tend to develop along different types by a priority sequence which reflects their mechanical strength. The development degree of BPFs also depends on the mechanical contrast with adjacent laminations; (2) When controlled by a single type of lamination, the density of BPFs increases with lamination density under a turning point and then decreases; (3) BPFs prefer to develop along the thinner lamination and are usually inside it, while controlled by thick lamination, BPFs tend to extend along the edge. The change in the thickness of laminations leads to a change in the development position of BPFs, indicating that the position of the weak plane controls the development position of BPFs; (4) When multiple types of lamination coexist, the type and thickness of laminations jointly influence the development of BPFs. Plastic thin laminations are conducive to the development of BPFs, while brittle thick laminations are not conducive. When the thickness of the plastic lamination is close to or less than that of the brittle, the influence of lamination type dominates BPFs, while the thickness of the

plastic laminations is much larger than the brittle, the influence of lamination thickness will dominate.

KEYWORDS

**bedding-parallel fracture, lamination, tight oil sandstone, upper Triassic Yanchang Formation, Ordos Basin**

# 1 Introduction

In recent years, with the increasing demand for oil and gas resources, the exploration and development of unconventional oil and gas have become a focus. Tight oil, a very important type of oil and gas, has received widespread attention (Zou et al., 2012). In recent years, China has made significant breakthroughs in the exploration and development of terrestrial tight oil, demonstrating good exploration prospects. Among them, the Chang7 section of the Ordos Basin, as one of the demonstration areas for tight oil exploration and development in China, has formed a typical source reservoir symbiotic oil reservoir with tight sandstone and organic-rich shale interlayers. The resource potential is enormous, and the geological reserves reach 2 billion tons. There is poor reservoir porosity and strong heterogeneity in tight sandstone reservoirs. Natural fractures makes a significant contribution to improving reservoir permeability and flow capacity (Anders et al., 2014; Sarhan and Selim, 2023). Natural fractures are important controlling factors for oil and gas enrichment and high production (Sarhan et al., 2017). Studying the distribution patterns of natural fractures is of great significance for promoting the exploration and developmentsri of tight oil (Dong et al., 2020; Dong et al., 2022; Dong et al., 2023; Sarhan et al., 2023; Dong et al., 2024).

Natural fractures mainly refer to macroscopic discontinuous structural features formed due to tectonic deformation or physical diagenesis. Natural fractures can be divided into structural fractures, diagenetic fractures, and abnormal high-pressure fractures, with diagenetic fractures further classified into BPFs and shrinkage fractures (Zeng et al., 2016; Zeng et al., 2021a). BPFs in tight sandstones are natural fractures that are formed along the bedding during the processes of sedimentation and diagenesis (Swanson, 2007; Zeng and Li, 2009). Laminations, as controlling factors for the development of weak planes in sandstone reservoirs, exhibit smaller-scale heterogeneity in their distribution. Even within the same lithofacies, lamination characteristics vary greatly. Zeng et al. (2022) proposed that laminations represent lithological interfaces and mechanical weak planes, more prone to compaction. It is suggested that the thinner the lamination, the higher the degree of development of BPFs. Feng et al. (2020) argued that BPFs are controlled by differences in lithology between laminations, with larger lithological differences leading to greater diagenetic shrinkage during compaction, and hence more developed BPFs. According to the findings of previous research (Zeng et al., 2021b; Xu et al., 2021), it has been established that the development of laminations inevitably impacts the development of BPFs. Due to the different mechanical properties of laminations, the type, density, and thickness of laminations are significant in controlling the development of BPFs (Fraino et al., 2022). BPFs play a dual role in reservoir geology. On one hand, they create additional pore space and enhance the hydrocarbon potential of reservoirs with well-developed BPFs (Luo et al., 2017; Pang et al., 2023; Zeng et al., 2024). On the other hand, they significantly increase permeability, particularly in the horizontal direction, thereby enhancing the flow capacity of reservoirs (Laubach and Diaz-Tushman, 2009; Cobbold et al., 2013). Therefore, studying the influence of laminations on the development of BPFs is of great significance for promoting the exploration and developmentsri of tight oil.

Utilizing core and thin section data, this study provides a detailed characterization of the development characteristics and distribution patterns of BPFs in the tight sandstone reservoir of the Upper Triassic Yanchang Formation in the Ordos Basin, China. By delineating the characteristics of laminations, similar and relatively homogeneous lamination units are selected as the measurement objects to investigate the impact of various lamination characteristics on the development of BPFs and the interrelationships when multiple characteristics coexist. The study aims to reveal the control of laminations on the development of BPFs in tight oil reservoirs. This research provides insights into the formation mechanisms of BPFs and offers guidance for the prediction and modeling of BPFs in tight oil reservoirs.

# 2 Geological setting

The Ordos Basin is located in the western part of the North China Craton. It is bordered to the north by the Yinshan Mountains, to the south by the Qinling Mountains, to the east by the Lvliang Mountains, and to the west by the Helan Mountains-Liupan Mountains. A large-scale inland depression basin developed under the impact of the Indosinian movement in the Paleozoic (Chen et al., 2011). According to its tectonic evolution history and current basin morphology, the Ordos Basin can be divided into six secondary tectonic units: the western thrust belt, Tianhuan depression, Yishan slope, Jinxi flexural fold belt, Yimeng uplift, and Weibei uplift. The basin exhibits an asymmetrical monocline with a steep slope to the southwest and a gentle slope to the northeast (Deng et al., 2008) as shown in Figure 1.

During the Middle-Late Triassic, the basin underwent an evolutionary cycle from rifting and expansion to extinction, depositing the Yanchang Formation of inland river-delta-lake facies. The deposition during the Chang 7 stage represents the peak period of the basin, forming a broad deep-lake to shallow-lake environment, with the deposition of a series of shale strata dominated by dark mudstone and black shale. Shallow water deltas developed at the southwestern and northeastern margins of the basin due to the influx of sediment from the source areas in these regions (Yang et al., 2013). In the later stages of the Chang 7 deposition, as the basin gradually contracted and the delta progrades, the frequent volcanic and seismic activities triggered

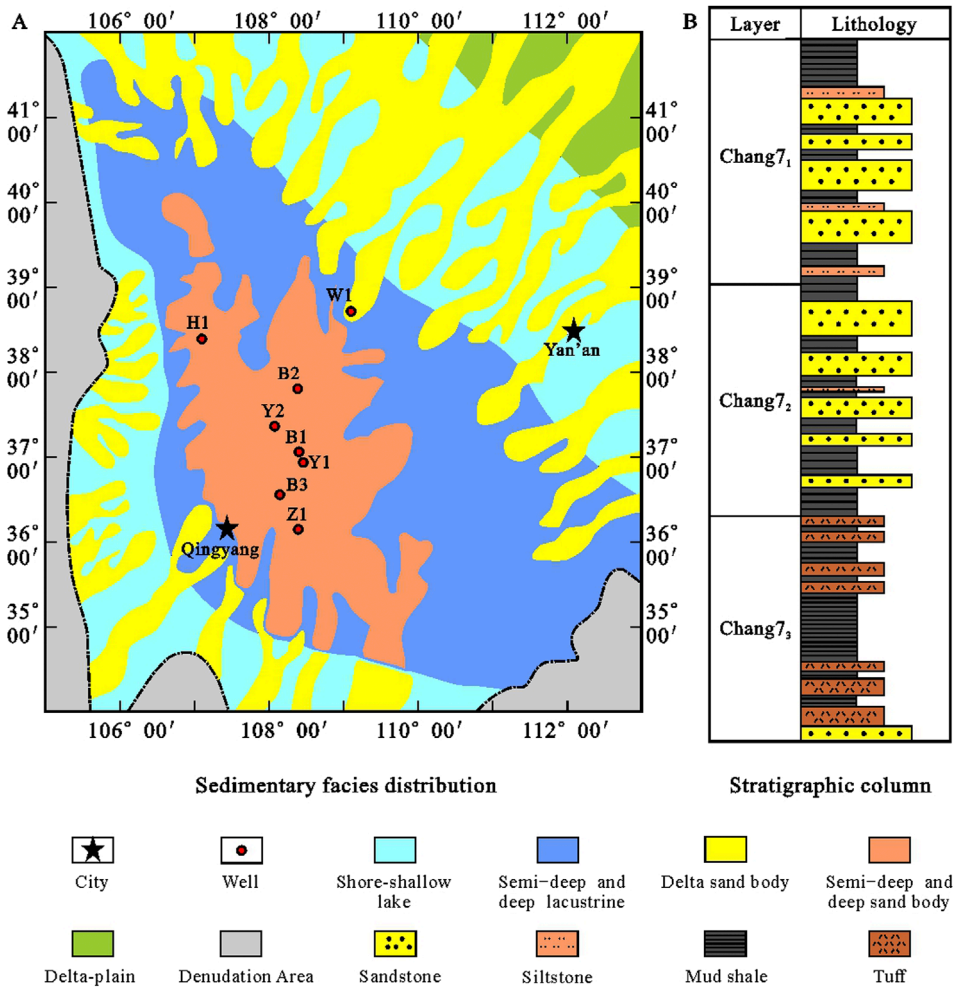


FIGURE 1
**(A)** Sedimentary facies and **(B)** stratigraphic column of the Chang 7 section in the Ordos Basin (Fu et al., 2020).

instability in the sediment of the delta front, resulting in gravity flows such as debris flows and turbidity currents in the central basin. This also led to the widespread development of tuffaceous interlayers and laminations of varying thickness (Chen et al., 2011; Li et al., 2022). Therefore, based on the vertical evolution characteristics of sedimentation and differences in lithology, the Chang 7 section is divided into three sub-sections. Among them, the Chang $7_3$ sedimentary period is the largest lake intrusion period, mainly composed of shale, while the Chang $7_1$ and Chang $7_2$ sub-sections are influenced by gravity flow, mainly composed of shale and tight sandstone interbedded.

The Chang 7 reservoir of the Yanchang Formation is characterized by sandstone at the top and predominantly black shale at the bottom (Figure 1). The porosity of the Chang 7 reservoir follows a normal distribution, primarily concentrated in the range of 6%–14%. The permeability is distributed within the range of (0.01–0.40)×10-3 μm$^2$, indicative of a typical tight oil reservoir. The natural fractures developed within the reservoir can provide migration pathways and storage space for the tight oil, effectively improving reservoir properties. This is beneficial for the development of tight oil resources in the Chang 7 reservoir of the Yanchang Formation in the Ordos Basin (Ju et al., 2020). Considering that the main exploration target of the Chang 7 reservoir is the upper section, this article focuses on the sandstone at the top of the Chang 7 reservoir and explores the influencing factors of reservoir fractures, to provide some reference for the exploration of tight oil in the Chang 7 section.

## 3 Samples and methods

In order to accurately investigate the development characteristics and patterns of lamination and BPFs, rock cores from the Chang 7 segment of eight wells in the Ordos Basin were selected for observation. The total length of the cores amounts to 359.42 m. Heterogeneity in the development of lamination and BPFs was observed in the tight sandstone. Some core intervals exhibit dense visible laminations and fractures, while others are relatively homogeneous. Based on systematic observations, representative segments with varying degrees of lamination development were selected for sampling, totaling 22 blocks. All samples were cut longitudinally and ground into thin sections perpendicular to

the bedding planes, and then filled with blue epoxy resin to enhance the visibility of the fractures. All casting thin section samples were observed and photographed under a polarizing microscope (Olympus BX51) to analyze the microscopic features of the lamination and BPFs. Additionally, continuous photographs along a vertical line perpendicular to the lamination were taken for individual samples to stitch together, enabling the complete documentation of the vertical distribution characteristics of the lamination and BPFs.

The aperture of the BPFs is measured under a microscope using the built-in measurement software tools. To reduce systematic errors and deviations caused by aperture variations, three random measuring points were selected for averaging in relatively stable sections of the BPFs. Since the thin sections were cut perpendicular to the bedding planes, the measured visual aperture can be treated as the true aperture. After the core is retrieved from underground to the surface, the decrease in confining pressure leads to a significant increase in the aperture of the BPFs. Therefore, it is necessary to correct these measurements to reflect the true underground aperture. The correction method involves restoring the measured aperture at the surface to the true aperture under subsurface confining pressure conditions based on the relationship between the fracture aperture and the static rock closure pressure.

In this study, the degree of BPFs development is characterized using two methods: linear density (P10) and area density (P21). By employing scanning and stitching methods, the distribution of fractures throughout the entire sample can be obtained, allowing for the calculation of the overall fracture density. P10 represents the number of fractures per unit length along a measuring line perpendicular to the fracture planes. For vertical wells, it is the ratio of the number of BPFs to the length of the core. Meanwhile, P21 is the ratio of the cumulative length of fractures within a vertical fractures plane to the total area of the plane. For nearly parallel BPFs, where the fractures have considerable length and do not terminate within the entire field of view, P10 suffices to adequately reflect the degree of fracture development. However, when fractures generally terminate within the field of view, the selection of the measuring line can influence the measurement results. In such cases, P21 is more reliable.

# 4 Results

## 4.1 The type and combined characteristics of laminations

### 4.1.1 Lamination types and development characteristics

In the Chang 7 tight sandstone reservoir, various types of lithologies exhibit widespread development of laminations. The types of laminations mainly include clay laminations, biotite laminations, organic laminations, and tuffaceous laminations. Laminations are formed by relatively homogeneous specific components, and when these components are vertically stacked and continuously separated by other components, they should be considered as multiple laminations.

Clay laminations develop in various lithologies and appear as brownish-brown under the microscope, with significant variations in thickness. In sandstone and siltstone, they are present as thin laminations sandwiched between sand laminations, with a low development frequency. In mudstone, they are developed overlapping with sand laminations of the same scale, with a similar development frequency (Figure 2G).

Organic matter laminations are extensively developed in the Chang 7 reservoir, but their development varies within different lithologies. The lateral continuity of organic laminations is good and extends over a considerable distance. Their morphology is closely related to lithology. In sandstone, they commonly exhibit undulating patterns (Figure 2C, D), indicating their sensitivity to depositional hydrodynamics (Nath and Mokhtari, 2018).

Biotite laminations are developed in fine sandstone and siltstone, appearing as light brown under the microscope, with thicknesses ranging from tens to hundreds of micrometers. The laminations are composed of single or multiple laminations of biotite, with grains exhibiting a distinct directional arrangement, their long axes are parallel to the layering, and the short axis grain size is approximately 30–200 μm. The distribution of biotite laminations is closely related to bedding planes; laminations extending parallel to the bedding planes exhibit a straight and continuous morphology (Figure 2B), while those distributed along oblique bedding planes show a low-angle staggered distribution, gradually curving and converging towards the lower boundary of the bedding planes. The continuity of single-lamination biotite laminations is related to grain size, with fine-grained laminations exhibiting lateral continuity and stable distribution, while laminations with a short-axis grain size greater than 120 μm appear to have varying degrees of discontinuity (Figure 2B). When a sufficient sediment supply allows for continuous deposition of multiple biotite laminations, the laminations maintain good continuity.

Tuffaceous laminations are primarily developed in fine sandstone, with thicknesses on the order of tens of micrometers, overlaying organic laminations, and clay laminations, and can also coexist at thicknesses of hundreds of micrometers with clay laminations (Figure 2F). Tuffaceous laminations consist of a combination of volcanic glass and crystal fragments in different proportions, and their morphology commonly exhibits curvature. The volcanic glass is distinguished from crystal fragments by its irregular chicken bone and crescent-shaped forms, and tuffaceous laminations with a high proportion of volcanic glass commonly experience devitrification. Some samples, after undergoing extensive weathering, have fuzzy grain edges and their original structures are no longer visible.

### 4.1.2 Lamination combination

The lamination combination is composed of specific types of laminations, but it does not reflect differences in lamination thickness, density, and other characteristics, all of which can affect the development of BPFs (Dean et al., 2001; Zhao et al., 2019). When these parameters change simultaneously, it is difficult to distinguish the differences in BPFs and their relation to specific parameters. Lamination and BPFs density reflect the average density within the measurement range, smoothing out differences within that range and failing to show the influence on the BPFs at that scale. Therefore, it is crucial to select an appropriate measurement unit. On one

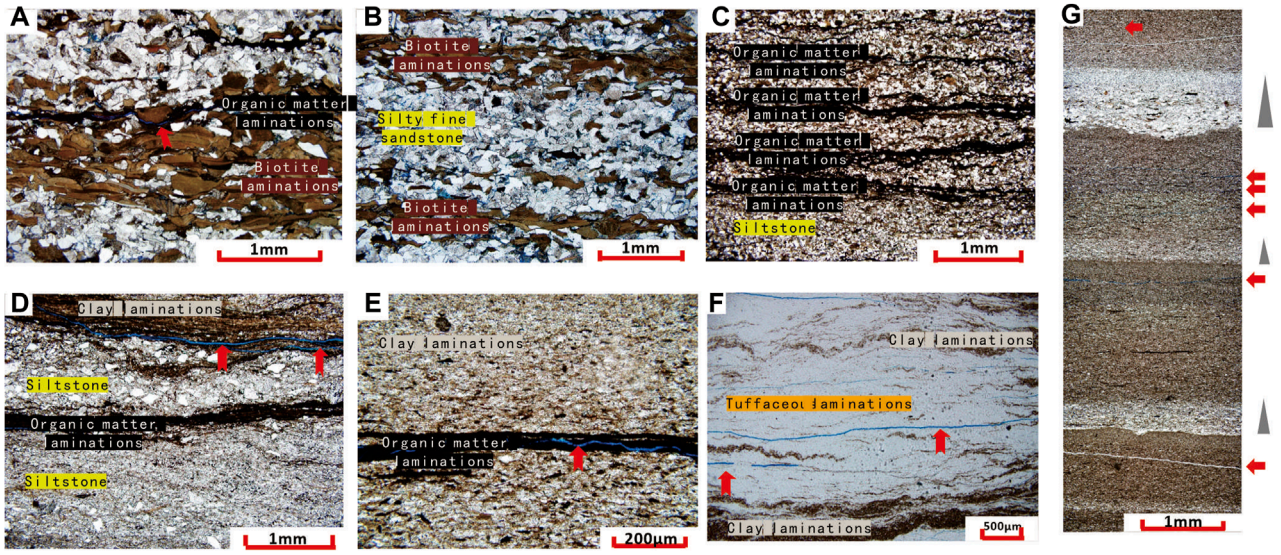


FIGURE 2
The lamination combination types in tight sandstone of the Chang 7 reservoir in the Ordos Basin. **(A)** Thick biotite laminations with interbedded thin organic laminations. BPFs develop along the organic laminations boundary, (Well W1, 2019.2 m, plane-polarized thin sections); **(B)** Fine sandstone with well-developed parallel bedding planes enriched with biotite. (Well W1,1991.8 m, plane-polarized thin sections); **(C)** Siltstone with wavy bedding planes enriched with biotite and organic matter, (Well W1,1977.5 m, plane-polarized thin sections); **(D)** Mudstone with interbedded clay laminations and silt laminations. BPFs develop along the boundaries of the clay laminations, (Well Y1,1931.25 m, plane-polarized thin sections); **(E)** Siltstone-mudstone with interbedded clay laminations and silt laminations, exhibiting granular lamination. BPFs develop along the boundaries of the clay and organic laminations, (Well Y2,1808.73 m, plane-polarized thin sections); **(F)** Tuffaceous laminations and clay laminations interbedding, with BPFs developing within the tuffaceous laminations, (Well B2,1963.23 m, plane-polarized thin sections); **(G)** Mudstone with interbedded clay laminations and silt laminations, exhibiting granular lamination. BPFs develop along the boundaries of the clay and organic laminations, (Well Y2,1808.73 m, plane-polarized thin sections); Blue indicates unfilled BPFs, red arrows indicate BPFs.

hand, it should have relatively stable lamination characteristics, and on the other, the distribution of laminations and BPFs within it should be relatively homogeneous. Based on the lamination combination, the parts with stable attributes such as lamination type, scale, and density can be divided into lamination combination units vertically, serving as the measurement unit for laminationsri characteristics (Figure 3).

Lamination combinations are developed by the vertical stacking of multiple laminations related to different origins. Each lamination combination has specific lamination types, structures, and features, reflecting relatively stable climatic, source input, and hydrodynamic conditions over a period (Sageman et al., 2003; Lazar et al., 2015; Gou and Xu, 2023). In the Chang 7 reservoir, the main lamination combinations include the biotite-organic, clay-organic, and clay-tuffaceous series.

The lamination combination of biotite-organic series is mostly in millimeter-scale thickness, characterized by the coexistence of biotite laminations and organic laminations. This feature may also be absent or undeveloped (Figure 2A–C). In lithologies with small grain sizes, the lamination exhibits a flat morphology with clear boundaries, while in lithologies with larger grain sizes, discontinuities appear at the boundaries of the biotite laminations, transitioning to sand facies. Laminations in parallel-laminated sandstone show good continuity and stable distribution, while in cross-laminated sandstone, the thickness of biotite laminations varies noticeably, displaying evidence of bending deformation.

The lamination combination of the clay-organic series varies in thickness from several hundred micrometers to millimeters, and it is developed by the overlapping of two types of laminations of similar scales (Figure 2D). The thickness of each type of lamination ranges from tens of micrometers to several hundred micrometers, with clear boundaries between adjacent laminations. In tight sandstone the clay laminations exhibit a flat and laterally stable morphology, while organic laminations may show lateral pinch-outs due to disturbance by large grain bioclasts or post-depositional water perturbation, resulting in poor continuity. In muddy siltstone, they display banded distribution due to water disturbance (Figure 2E).

The lamination combination of the clay-tuffaceous series exhibits significant differences in thickness, lamination thickness, and the ratio of the thickness of the two types of laminations, which are related to the relative strength of terrestrial supply and volcanic activity. The light-colored or variegated tuffaceous laminations have clear boundaries with the dark-colored clay laminations but exhibit different degrees of bending deformation, showing banded distribution and potential lateral pinch-outs (Figure 2F). This combination has low organic matter content, which is mostly dispersed within the clay laminations, and there is almost no organic matter in the tuffaceous laminations.

In some cases, there is a certain correspondence between lamination combinations and lithology, for example, the biotite-organic series is a typical lamination combination in fine sandstone and siltstone, and the clay-tuffaceous series constitutes the main part of the tuffaceous rock. However, lamination combinations developed in different lithologies also intersect and overlap. For example, the clay-organic series is commonly developed in muddy siltstone and silty mudrock and is also present in some

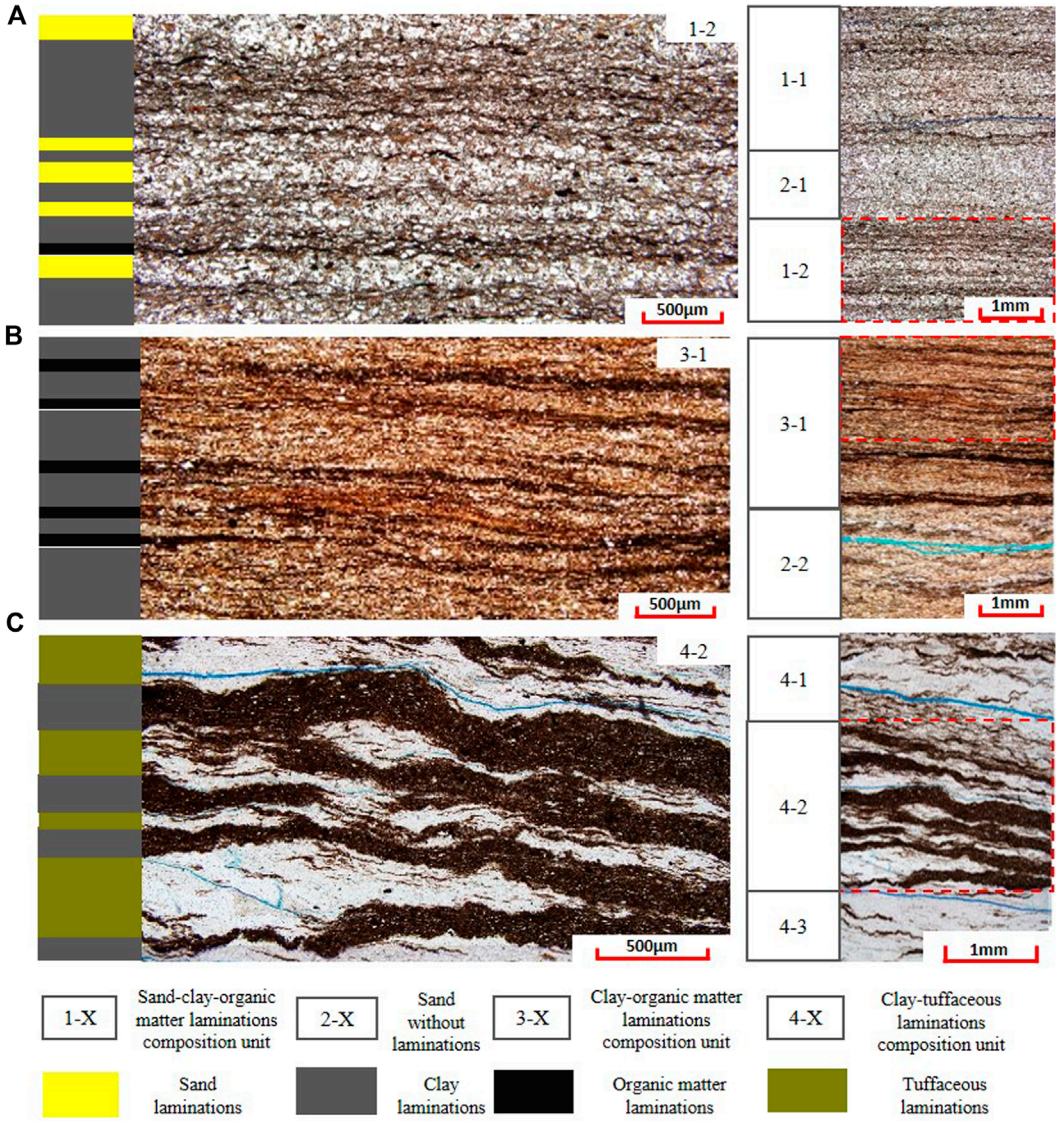


FIGURE 3
Example of division of lamination combination units. **(A)** Sand-biotite-organic matter combination unit (Well W1,2001.25 m); **(B)** Sand-clay-organic matter combination unit (Well B3, 1960.1 m); **(C)**. Clay-tuffaceous combination unit (Well B2,1963.23m).

calcareous tuffaceous rocks. These lamination combinations, as units that constitute the rock, overlap in different proportions during the cyclical changes in sedimentary conditions, resulting in diverse lithologies (Schieber, 2011; Gorniak, 2017). Further analysis at a smaller scale reveals that lamination combinations are controlled by the formation of causally related laminations, leading to heterogeneity at different scales. Therefore, the reservoir characteristics related to it (such as BPFs) are essentially controlled by the lamination and its combinations.

## 4.2 Characteristics of BPFs

BPFs are natural fractures formed in rock due to the failure of bedding planes. In oil-bearing sandstone, the seepage of oil along the BPFs can indicate their presence (Figure 4). In petrographic thin sections, the BPFs filled with blue resin show significant contrast with the surrounding rock, making it easy to distinguish them from unbroken bedding planes. Microscopic observations reveal that BPFs develop in various types of laminations, occurring both within the laminations (Figure 5B) and along the boundaries of the laminations (Figure 5C). The characteristics of BPFs are controlled by the laminations, and their distribution exhibits parallel or wedge-shaped interlocking features depending on the structure of the lamination combination (Figure 5A). As a result of lamination deformation, branching, thinning, and pinch-outs, BPFs also undergo deformation and termination (Figure 5B, C). Within the same lamination, irregular particle arrangement or later deformation can lead to the termination of BPFs, resulting in lower continuity and scale compared to the laminations.

In the Chang7 reservoir, the majority of BPFs are unfilled, accounting for over 95%, with only a few being locally filled

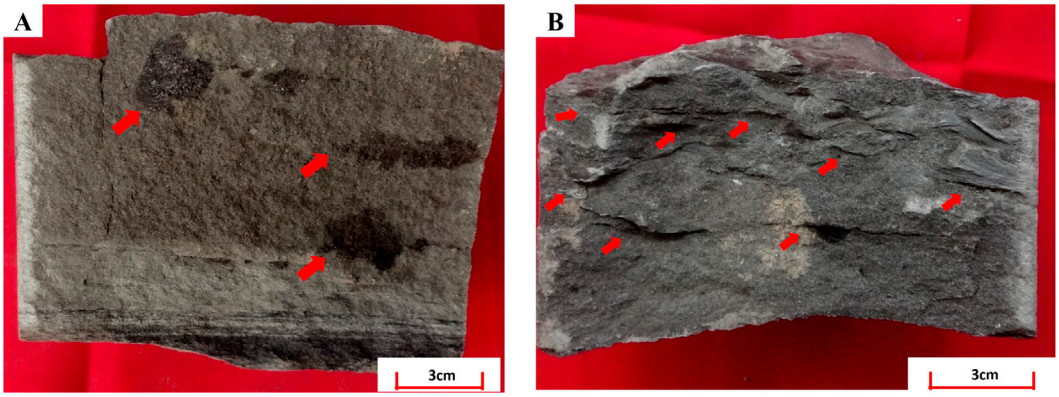


FIGURE 4
Bedding-parallel fractures in tight sandstone core of the Chang 7 reservoir in the Ordos Basin, oil exudes along bedding-parallel fractures. **(A)** Well Z1, 1664.2 m. **(B)** Well Z1, 1666.4 m. Red arrows indicate bedding-parallel fractures.

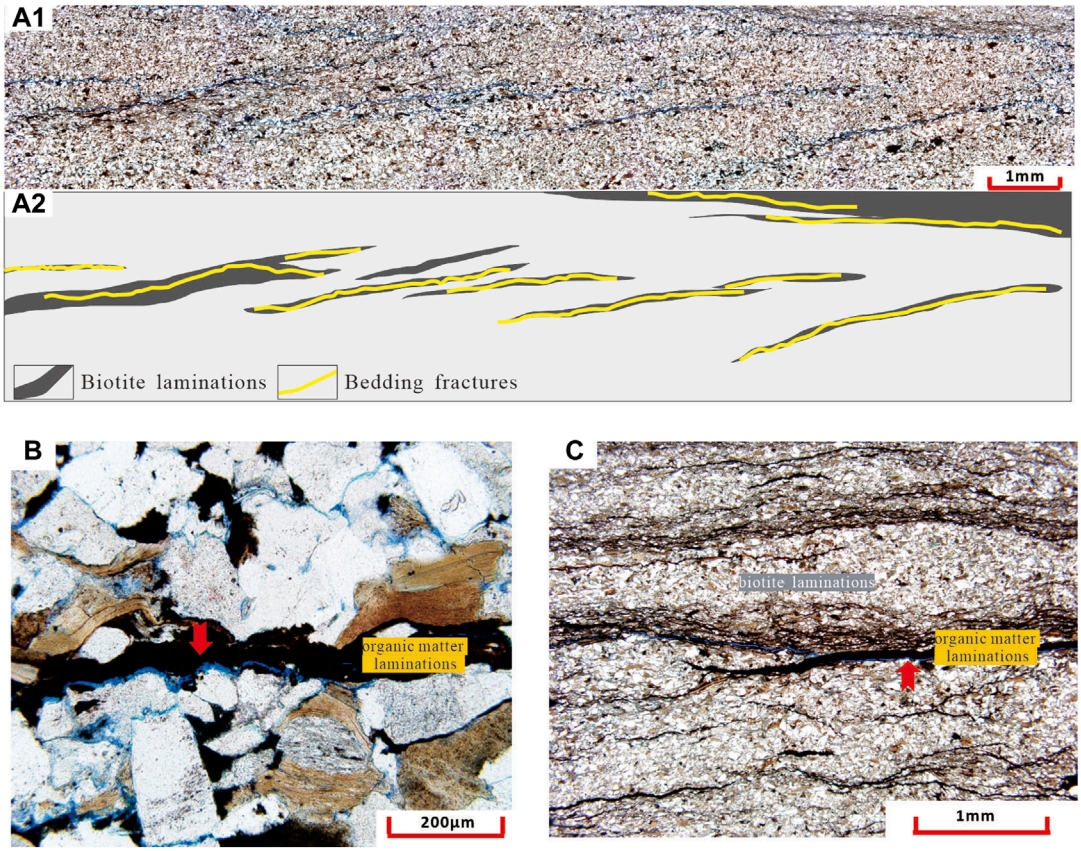


FIGURE 5
Morphological characteristics of bedding-parallel fractures in tight sandstone of the Chang 7 reservoir in the Ordos Basin. **(A1)** BPFs develop along the biotite laminations, with unfilled fractures marked in blue (Well W1,1999.5 m, plane-polarized thin sections), **(A2)** a sketch of **(A1)**, the biotite laminations in black and the BPFs in yellow. **(B)** BPFs develop along the edges of organic matter laminations, with unfilled fractures shown in blue (Well B1,1960.1 m, plane-polarized thin sections). **(C)** BPFs develop along the boundaries of biotite and organic matter laminations, where the laminations pinch out and the BPFs terminate. (Well W1,2005.4 m, plane-polarized thin sections). Red arrows indicate BPFs.

with calcite and asphalt, while completely filled BPFs are rare, comprising only 3.4% (Figure 6). BPFs underground are subject to overlying rock pressure, and maintaining a significant aperture is challenging in the absence of pore fluid overpressure support. After correction, the underground aperture of BPFs is generally less than 40 μm, with 88% of them falling within the range of 0–10 μm (Figure 6A). The filling nature of BPFs varies with different apertures; those with apertures of 10–30 μm exhibit a higher

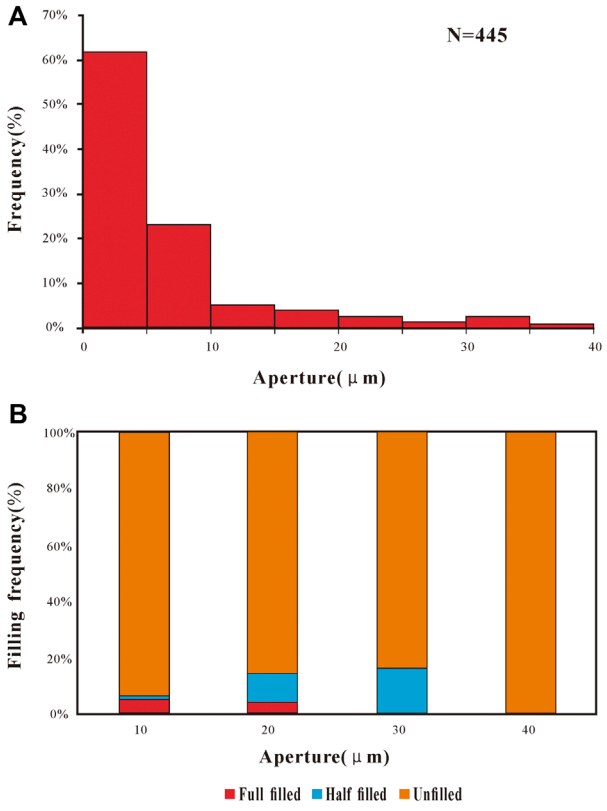


FIGURE 6
The aperture and filling property of bedding-paralleled fractures in the Chang 7 reservoir of the Ordos Basin. **(A)** Aperture distribution of bedding-paralleled fractures. **(B)** Filling property of bedding-paralleled fractures with different aperture.

filling proportion, while those with apertures exceeding 30 μm are generally unfilled (Figure 6B).

The development of BPFs is influenced by rock composition and structure (Abaab et al., 2021). Brittle minerals increase the brittleness of the rock, making it more prone to fracturing under external forces; organic matter, through hydrocarbon generation, can create abnormally high pressure, leading to tensile fracturing by converting the stress on the rock into a tensile state; weak planes between lamination provide the basis for the formation of BPFs (Ojala and Tiljander, 2003). These features are inherently contained within the lithology, and thus, the degree of BPFs development is expected to vary with different lithologies.

The measurement results indicate that the development of BPFs in muddy sandstone is significantly higher compared to other lithologies, with a $P_{10}$ of up to 0.6 $mm^{-1}$ and a $P_{21}$ of approximately 0.45 $mm^{-1}$. In contrast, the $P_{10}$ and $P_{21}$ of BPFs in other lithologies range from 0.27 to 0.32 $mm^{-1}$ and 0.26 $mm^{-1}$ (Figure 7).

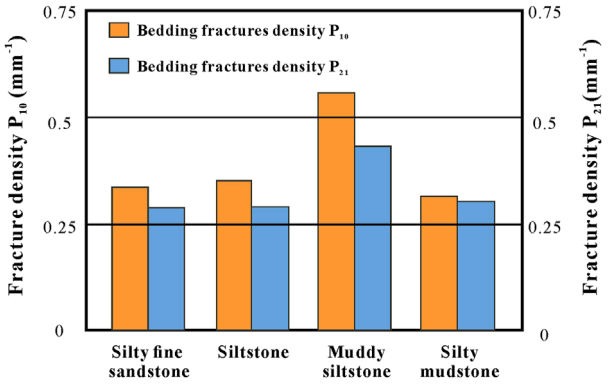


FIGURE 7
Density of BPFs in different lithologies in the Chang 7 reservoir in the Ordos Basin.

# 5 Discussions

## 5.1 The influence of lamination types on the development of BPFs

In lamination combinations with multiple types of laminations, BPFs tend to develop along a specific type of laminations (Figure 3).

When laminations of sand overlap with clay laminations, BPFs only develop within the clay laminations, and their extent is also restricted by the clay laminations (Figure 8A). In combinations of clay and organic matter laminations, BPFs develop along the organic matter laminations. When organic matter coexists with biotite laminations, sandwiched between sandy interlayers, BPFs tend to extend along the biotite laminations rather than the organic matter (Figure 8B). Similarly, when organic matter laminations coexist with tuffaceous laminations, such as crystal pyroclasts, the BPFs do not develop along the organic matter laminations, but only along the crystal pyroclast laminations. Therefore, BPFs exhibit a priority sequence in different types of laminations: tuffaceous and biotite laminations are the highest priority, followed by organic matter laminations and then clay laminations.

In sandstones, BPFs commonly develop along biotite and clay laminations. However, in cases where laminations are discontinuous or absent, even with a high content of brittle minerals, it is difficult for BPFs to form (Figure 8I). The density of BPFs in sandstones is lower than in mudstones with less brittle mineral content, but with more pronounced laminations structures (Figure 2D, G), reflecting that the influence of laminations structures on BPFs is far greater than the influence of brittle mineral content. Organic matter hydrocarbon generation partly provides the dynamic conditions for the formation of BPFs but is not a necessary condition for their development. In organic matter-deficient sandstones, numerous BPFs are associated with biotite laminations, far exceeding the amount found in mudstones with higher organic matter content but lacking lamination structures (Figure 4A). Even within organic matter, fragments of higher plants and inertinite do not possess hydrocarbon generation potential, and only develop BPFs when present as laminations (Figure 8H). The development of BPFs within laminations also exhibits significant differences. BPFs are typically more easily developed in continuous and dense laminations (Figures 2E, 8D), whereas in some samples with partially continuous laminations, BPFs may not develop (Figure 2B, C). Instead, they are highly developed in laminations with poor continuity or isolated distribution (Figures 4A, 8C), demonstrating the complex impacts of lamination types on BPFs.

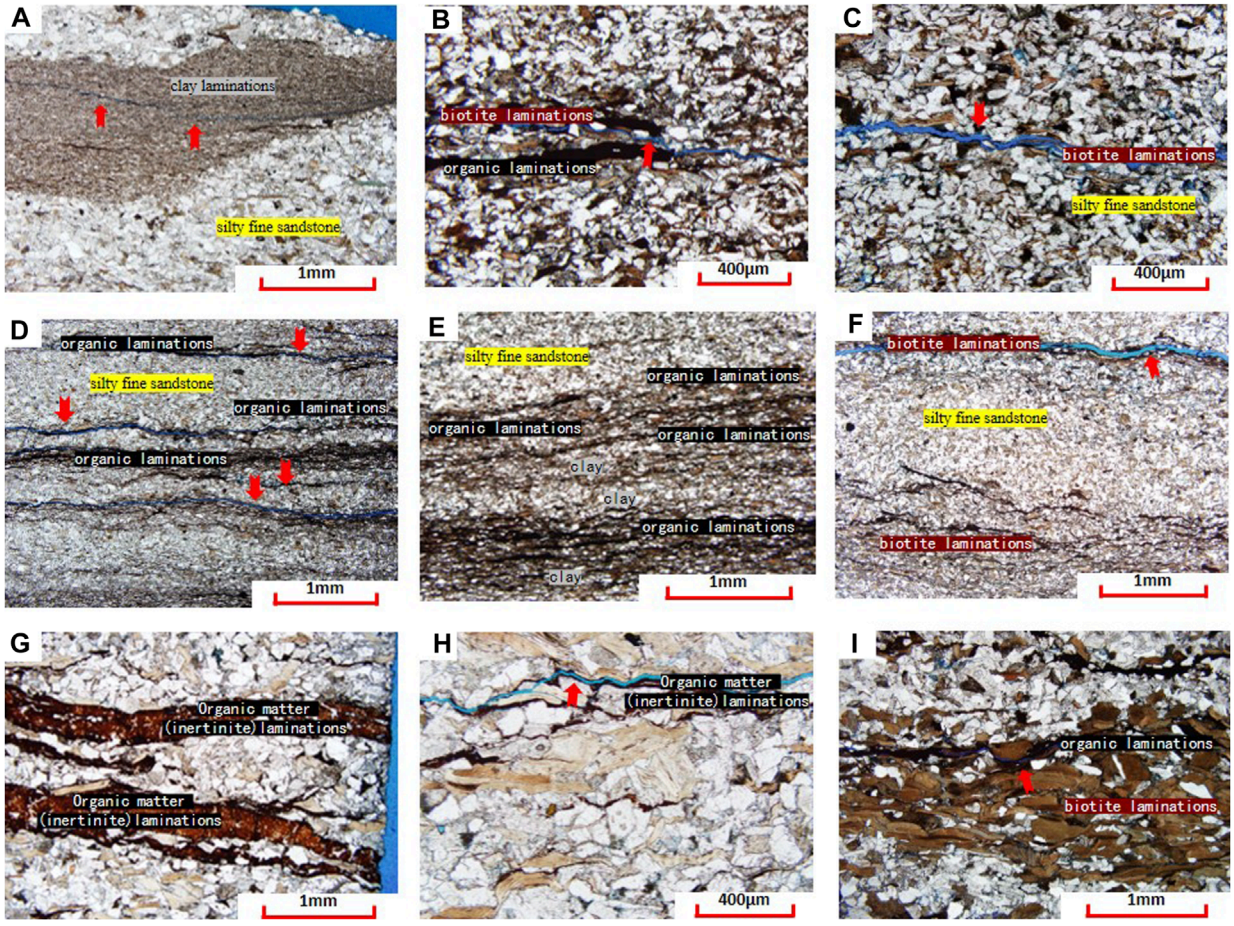


FIGURE 8
The development characteristics of fractures in the tight sandstone of the Chang 7 reservoir in the Ordos Basin. **(A)** BPFs develop along clay laminations (Well Y1,1931.25 m, plane-polarized thin sections). **(B)** BPFs develop along biotite laminations rather than organic matter laminations (Well W1,1990.3 m, plane-polarized thin sections). **(C)** Discontinuous biotite laminations overlaid with fine sand laminations develop BPFs (Well W1,1990.3 m, plane-polarized thin sections). **(D)** BPFs develop in organic matter laminations overlaid with fine sand laminations (Well W1, 2001.25 m, plane-polarized thin sections). **(E)** BPFs do not develop in organic matter laminations coexisting with clay (Well W1, 1987.4 m, plane-polarized thin sections). **(F)** BPFs develop along thin biotite laminations rather than thick ones. (Well W1,1994.93 m, plane-polarized thin sections). **(G, H)** BPFs develop along thin organic matter (inertinite) laminations rather than thick ones (Well W1, 2009.4 m, plane-polarized thin sections). **(I)** In thick biotite laminations, thin organic matter laminations are sandwiched, and BPFs develop along the organic matter laminations (Well W1, 2019.2 m, plane-polarized thin sections). Blue arrows indicate unfilled BPFs and red arrows indicate BPFs.

BPFs are not solely controlled by a single type lamination, but can also be controlled by two or more types of laminations (Figure 9). For example, in clay-organic matter lamination combination and organic matter-biotite lamination combination, bedding-parallel fractures can be controlled by multiple types of laminations. Measurement and analysis of such multiple-types-lamination-controlled lamination combinations (Figure 10) reveal that in the combination of organic matter and clay laminations, when the density ratio of organic matter laminations to clay laminations is greater than 0.8, high-priority organic matter laminations dominate the development of BPFs, with only a few fractures developing along the clay laminations, and the ratio between the two can exceed four times; when the density ratio of the two laminations drops to 0.3, the proportion of BPFs developing along the organic matter laminations significantly decreases, with more BPFs developing along the clay laminations, and the density of BPFs developed in the two laminations becomes similar. Similar patterns are also observed in the combination of biotite-organic matter laminations; when the density ratio of biotite laminations to organic matter laminations is greater than 0.8, the density of BPFs developed along the biotite laminations is more than twice that of the fractures developed along the organic matter laminations, and when the density ratio drops to around 0.2, the density of BPFs developed along the two types of laminations becomes comparable. In conclusion, only when high-priority laminations reach a certain proportion can they dominate the distribution of BPFs; below this proportion, the development of BPFs in low-priority laminations significantly increases.

The difficulty of fracturing along laminations as mechanical weak planes depends on the strength of the laminations. When multiple laminations coexist, external forces tend to cause fractures

along the weakest plane, generally in the direction of the lowest strength, leading to a priority sequence in the development of BPFs. This priority sequence reflects the increasing vertical strength from tuffaceous lamination and biotite lamination to sand lamination. Therefore, in cases where plastic laminations reach a certain proportion, BPFs are always predominantly controlled by the plastic laminations. However, when the number of plastic laminations is low, their fracturing may not be sufficient to release all the strain energy under external force, thus leading to additional fracturing in brittle laminations and the formation of BPFs.

In units controlled by a single type of lamination, bedding-parallel fractures are only influenced by this lamination. The ratio of the number of bedding parallel fractures to the number of corresponding laminations (i.e., development intensity) reflects the mechanical property of the lamination itself. Mineral particles are bonded together by intergrowths and cement (Farouk et al., 2024). The contact surface, as weak plane, determining the strength of the lamination. Tuffaceous laminations, formed by rapid sedimentation, lack other filling materials and cementation is insignificant. Therefore, the strength of tuffaceous laminations is lower than that of other mineral laminations. Organic matter laminations do not have contact surfaces with mineral particles, and their strength depends on the inherent strength of the organic matter. Despite the lower strength of organic matter, when it accumulates into a certain thickness of lamination, it can dissipate strain energy through plastic deformation and is less prone to fracturing. Therefore, even though organic matter laminations are not the toughest, they exhibit the lowest intensity of BPFs development.

The difficulty of development of BPFs also depends on the coexisting laminations. When biotite laminations coexist with sand laminations, even with poor continuity or a gap between biotite particles greater than the particle length, BPFs can still develop, linking the discrete biotite particles together (Figure 8C). When organic matter laminations develop independently in sand laminations, even with a small thickness, continuous BPFs can still form, and the development intensity is higher (Figure 8D); however, when organic matter coexists with clay laminations, it is difficult to form BPFs, even if they are densely stacked (Figure 8E). Therefore, the greater the difference in the mechanical properties of adjacent laminations, the easier it is to fracture along the weak planes, and the higher the development intensity of BPFs in plastic laminations.

## 5.2 The influence of lamination density on the development of BPFs

In the various types of lamination combinations within the Chang 7 reservoir, the scale and density variations of the biotite-organic matter lamination combinations demonstrate the significant differences in lamination characteristics. The laminations exhibit a relatively flat and horizontally stable distribution, making the influence of lamination morphology on the development of bedding-parallel fractures is negligible. Therefore, the impact of lamination density on the development of BPFs is discussed through the biotite-organic matter lamination combination.

As mentioned above, in units with multiple laminations control, the strength of lamination itself and the interaction with adjacent

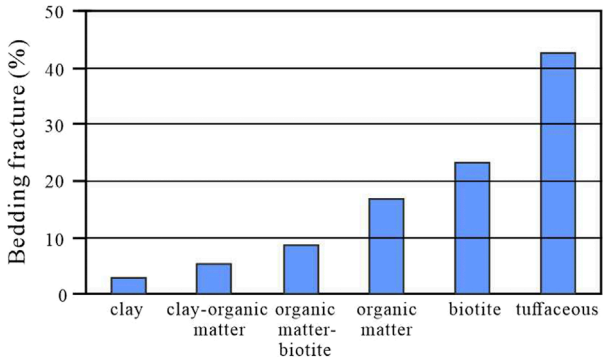


FIGURE 9
The percentage of BPFs controlled by different kinds of lamination.

lamination, collectively leading to differences in the development intensity of BPFs for different types of laminations. Therefore, only in units controlled by a single type of lamina is it possible to exclude the mutual influence of different laminations and demonstrate the relationship between lamination properties and the development of BPFs.

In the combination of biotite-organic matter laminations developed in tight sandstone, BPFs are respectively dominated by two types of laminations: biotite and organic matter. In units controlled by biotite laminations, the $P_{10}$ of biotite laminations ranges from 1–30 $mm^{-1}$, while the developed BPFs $P_{10}$ ranges from 0.09–1.4 $mm^{-1}$. Except for two sample points, as the dominant lamination density increases, the BPFs density shows an initial increase followed by a decrease, with the highest value appearing at a lamination density $P_{10}$ of around 6 $mm^{-1}$, at which point the BPFs density $P_{10}$ reaches 0.8 $mm^{-1}$ (Figure 11A). Units controlled by organic matter laminations exhibit a similar pattern, with the highest value occurring at a lamination density $P_{10}$ between 5–10 $mm^{-1}$ (Figure 11B).

The weak planes between lamination are the source of micro-cracks under stress loading (Cheng et al., 2024), thus the fracture density should increase with lamination density. According to previous studies, the primary driving force behind the formation of BPFs was the hydrocarbon generation caused by organic matter overpressure. It was also suggested that dense laminations typically reflect a more turbulent, oxygen-rich ancient aquatic environment or seasonal input of terrigenous material, which is unfavorable for organic matter enrichment and thus inhibits the formation of BPFs. (Xu et al., 2021; Zhao et al., 2021). In organic-poor sandstone, it is clear that the development of BPFs is not driven by hydrocarbon generation within the sandstone. Therefore, differences in hydrocarbon generation due to organic matter content are not the reason for this pattern. The formation of BPFs depends not only on the driving force of fractures but also on the mechanical properties of the laminations. When the lamination density is low, the development of BPFs increases with the increase in lamination density. However, when the lamination density is high, plastic laminations dissipate some strain energy through plastic deformation, leading to a reduction in the degree of fractures.

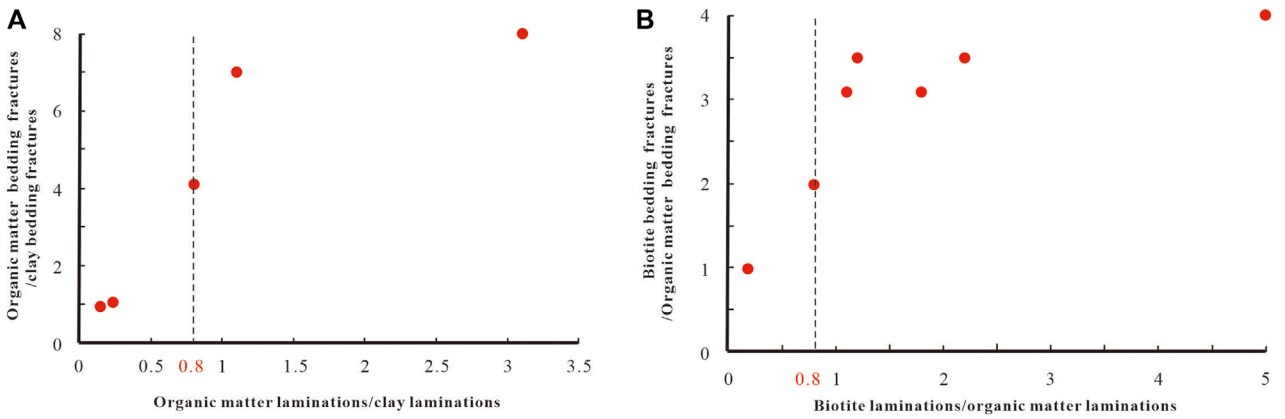


FIGURE 10
Density ratio of co-existing lamination and density ratio of related BPFs in lamination combination units controlled by multiple types of lamination. **(A)** Organic matter-clay. **(B)** Biotite- organic matter.

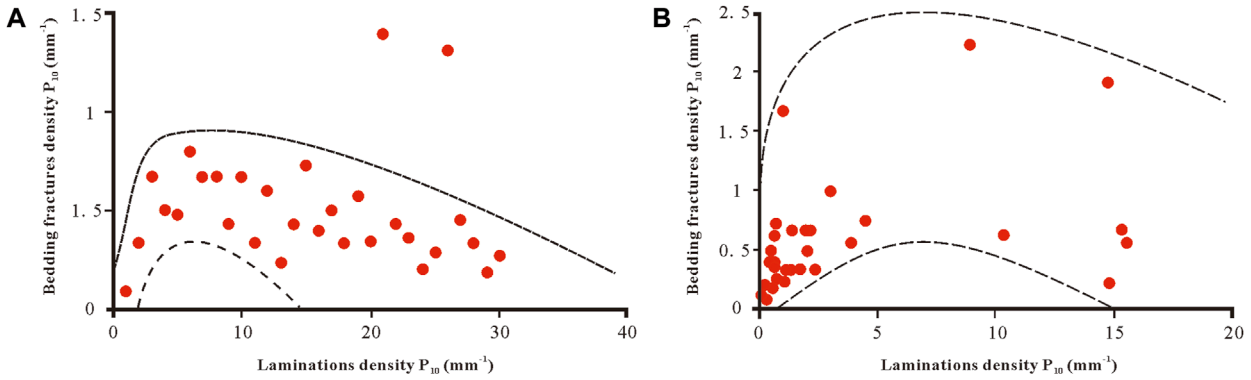


FIGURE 11
Relationship between bedding-parallel fractures density and laminations density in lamination combination units controlled by single type of lamination. **(A)** Biotite laminations. **(B)** Organic matter laminations.

## 5.3 The influence of lamination thickness on the development of BPFs

The thickness of laminations affects the development of BPFs in two ways. When the dominant laminations controlling the BPFs have a thickness similar to that of other non-dominant laminations, the spacing between the laminations is approximately equivalent to the lamination thickness. As a result, the laminations density is the reciprocal of the laminations thickness: the smaller the thickness, the greater the density, hence affecting the density of BPFs. However, when there is a significant difference in thickness between the dominant laminations and other laminations, the thickness no longer correlates with density, and can independently influence the development of BPFs. In the biotite-organic matter lamination combination, BPFs consistently develop along the thinnest lamination (Figure 8F). Similarly, when organic matter becomes the dominant laminations, BPFs also develop in relatively thinner laminations, whereas thicker laminations exhibit minimal development of BPFs (Figure 8G, H). This tendency is common in the biotite-organic matter lamination combination in sandstone, while in other lamination combinations, it is less pronounced due to other factors (such as lamination type) obscuring it.

The thickness of laminations also affects the development characteristics of BPFs. In the B2-3 sample, tuffaceous laminations and clay laminations are intercalated with significant lateral variations in lamination thickness: the laminations are thicker on the left side and thinner towards the right. Two different observation locations were selected on each side to obtain longitudinal sections A and B (Figure 12A, B). The laminations density in section A is slightly smaller than in section B, while the density of BPFs is significantly lower in section A compared to section B (Figure 12C). At the same time, the BPFs in section A exhibit larger apertures, with most exceeding 4 μm, while in section B, the apertures of BPFs are concentrated between 1 and 5 μm (Figure 12D). Due to the opposite differences in aperture and density, the cumulative aperture differences of the BPFs are minished with measured values along lines A and B being 114 μm and 168 μm, respectively. Consequently, in thicker laminations, BPFs develop in the form of low-density, large apertures, while in thinner laminations, they develop in the form of high-density, small apertures, maintaining relative stability in lateral strain.

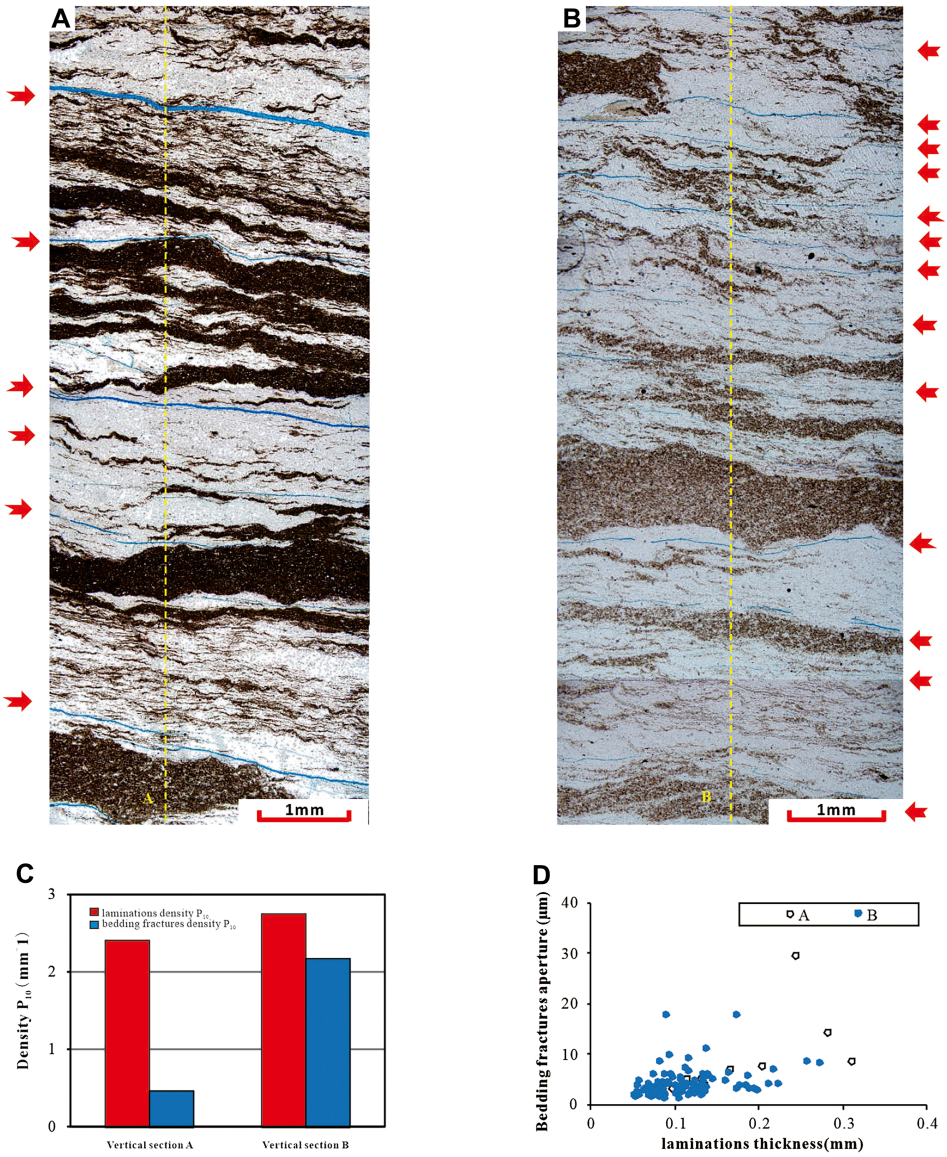


FIGURE 12
The relationship between the density and aperture of bedding-parallel fractures and lamination thickness in sections A and B. **(A)** Vertical section A (yellow dashed line represents the measuring line); **(B)** Vertical section B (yellow dashed line represents the measuring line); **(C)** The density of laminations and BPFs in two sections **(D)** The aperture of BPFs and the thickness of the laminations in two cross-sections. (tuffaceous laminations, Well B2, 1963.23 m) Red arrows indicate BPFs.

In laminations of different thicknesses, the development position of BPFs exhibits significant differences. In thin laminations (with thickness similar to the order of BPFs aperture), the BPFs develop within the laminations, while in thick laminations (with thickness considerably different from the order of BPFs aperture), the BPFs generally develop along the boundaries of the laminations. When a single lamination undergoes substantial thickness variation, the development position of BPFs also changes accordingly (Figure 5A). In lamination combinations, when a plastic lamination exists with a thickness much smaller than that of brittle laminations, its thickness can be neglected and the laminations themselves become the plastic surface within the rock. However, when the plastic lamination thickness is significant, the boundary of the laminations becomes more fragile compared to the homogeneous interior of the laminations. Thus, the position of the plastic surface controls the development position of BPFs. Statistical analysis regarding the relationship between the development of BPFs and the position of laminations of different thicknesses within various lamination types confirms this pattern. For laminations types, when the thickness of organic matter and biotite laminations, both being the primary carriers of BPFs, is below 0.2 mm, the BPFs generally develop within the laminations, while in laminations above 0.2 mm, the BPFs generally develop along the boundaries of the laminations (Figure 13B, C). Although the sample size for clay laminations is limited, it still shows similar differences (Figure 13A). It is noteworthy that the thickness of tuffaceous laminations does not

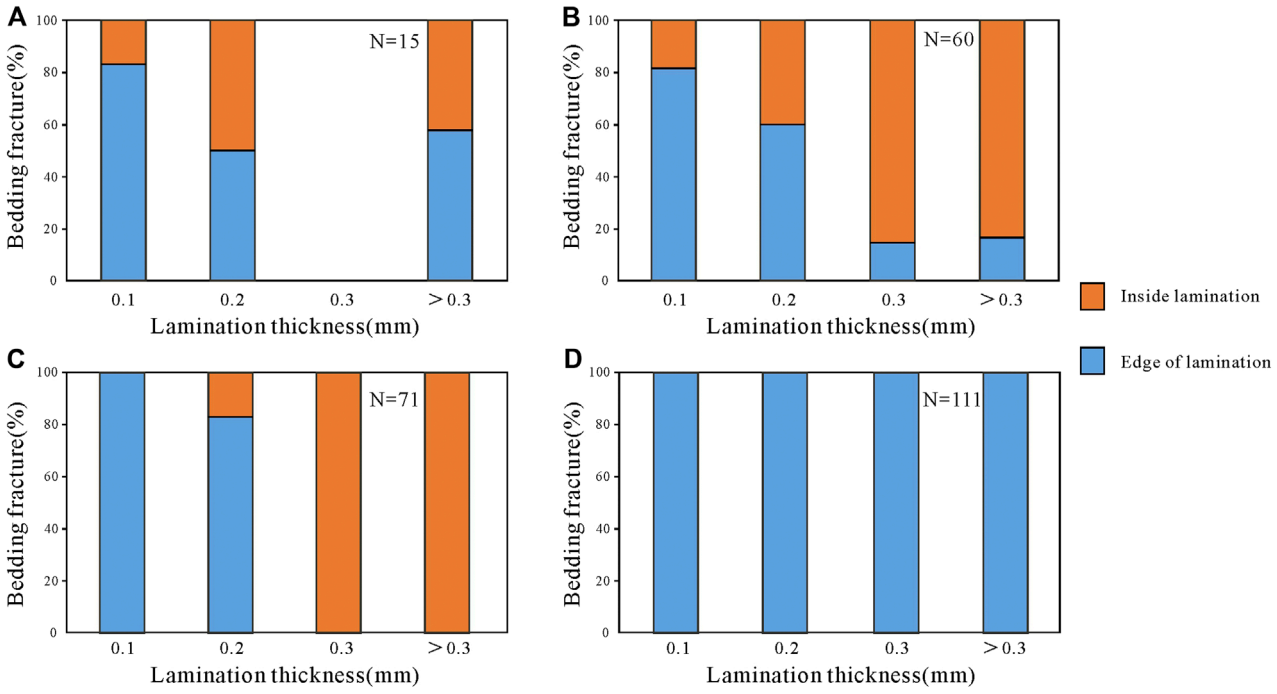


FIGURE 13
The development position of BPFs in laminations with different thickness **(A)** clay laminations; **(B)** organic matter laminations; **(C)** biotite laminations; **(D)** tuffaceous lamination.

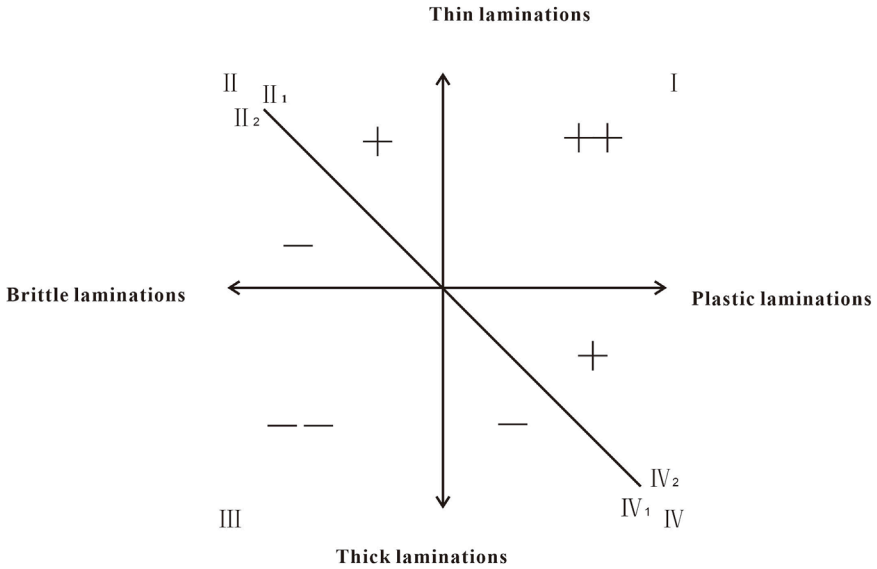


FIGURE 14
Diagram showing the influence of mechanical property and thickness of lamination on the development tendency of bedding-parallel fractures. + and – represent the relative development preference of bedding-parallel fractures. The quantity of + and – represents the degree of this preference of bedding-parallel fractures. The plastic thin lamination has the highest development priority, followed by brittle thin lamination and plastic thick laminations.

affect the development position of BPFs; all BPFs develop within the laminations (Figure 13D). This may be related to its low strength: there is no significant difference between the interior and boundaries of the laminations, and therefore the BPFs no longer tend to develop along the boundaries of the laminations.

## 5.4 The influence of lamination combination on the development of BPFs

The mechanical properties and thickness of laminations both influence the development tendency of BPFs. In lamination

combinations, the mechanical properties (relative strength) and thickness of coexisting laminations both have an impact, and different combinations can make the development pattern of BPFs more complex (Figure 14). When brittle thick laminations and plastic thin laminations coexist, both plasticity and thinness are favorable conditions for the development of BPFs, and these two factors have a similar impact (co-phase combination). As a result, BPFs naturally develop along the plastic thin laminations (quadrants I and III). On the other hand, when brittle thin laminations and plastic thick laminations coexist, plasticity is favorable for the development of BPFs, but thickness is not. This creates a competition between the two (quadrants II and IV), as the mechanical properties and thickness have opposite effects on the development of BPFs (antiphase combination). If lamination thickness has advantages, the bedding-parallel fractures tend to develop along the brittle thin laminations (quadrant II1). Conversely, if the mechanical property has advantages, the bedding-parallel fractures tend to develop along the plastic thick laminations (quadrant IV2). Due to the opposite effects of mechanical property and thickness, the development tendency of BPFs in antiphase combination may be indistinctive: both types of laminations develop BPFs, but more BPFs develop in one of the lamination types.

For example, in the biotite-organic matter lamination combination, the thickness of both the biotite laminations and organic matter laminations varies significantly, often resulting in the occurrence of organic matter thin laminations (relatively tough) adjacent to biotite thick laminations (relatively weak). In some cases, when the thickness difference between the two types of laminations is not large, the BPFs develop along the relatively weak biotite laminations, indicating that the mechanical properties of the laminations predominate. In most cases, extremely thin organic matter laminations coexist or are interspersed within the thicker biotite laminations, with the thickness of the biotite laminations being much greater than that of the organic matter laminations. Even if the organic matter laminations have a wavy morphology and poor continuity, which is unfavorable for the extension of BPFs, the BPFs strictly develop along the tougher but thinner organic matter laminations rather than the more continuous and weaker biotite laminations (Figure 8I). In these cases, lamination thickness has advantages in competition, overriding the influence of the mechanical properties in controlling the development tendency of BPFs.

Measurements and statistics were carried out on three fine sandstone samples from the same well, vertically distributed within a continuous sand body. The results confirmed this point. All three samples consisted of a combination of biotite and organic matter laminations, with similar lamination characteristics but significant differences in lamination thickness. The biotite laminations were thicker than the organic matter laminations, forming an antiphase combination. In sample W1-20, the average thickness ratio of biotite laminations to organic matter laminations was relatively small, and BPFs developed along the biotite laminations, indicating the dominance of mechanical property. Conversely, in samples W1-18 and W1-21, the thickness ratio of the two types of laminations is greater than 4, and more BPFs developed in the organic matter laminations, indicating the dominance of laminations thickness (Figure 15). Therefore, for this type of lamination combination, the critical lamination thickness ratio required for

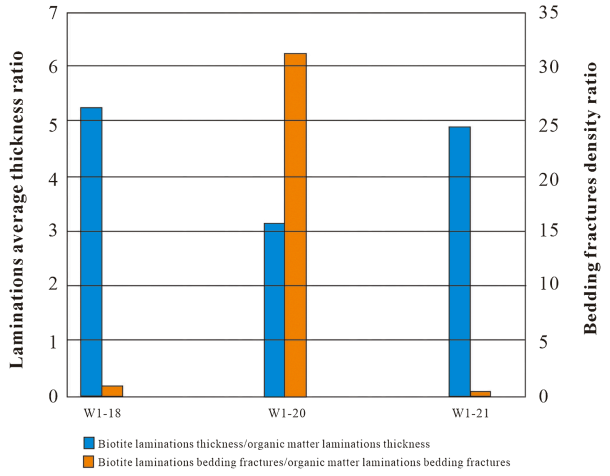


FIGURE 15
The development tendency of corresponding BPFs under different thickness ratios of biotite laminations/organic matter laminations.

lamination thickness to dominate is approximately between 3–4. It is noteworthy that near this critical value, as the laminations thickness ratio increased from 3.12 to 4.89, the density ratio of BPFs developed in the two types of laminations rapidly decreased from 31 to 0.07, indicating that the tendency of BPFs development is highly sensitive to changes in laminations thickness, and therefore the influence of laminations thickness on the development of BPFs cannot be ignored.

## 6 Conclusion

(1) The seventh member of the upper Triassic Yanchang Formation in the Ordos Basin mainly consists of tight oil sandstones, which are characterized by the development of clay laminations, organic matter laminations, biotite laminations, and tuffaceous laminations. The combinations include biotite-organic matter laminations, clay-organic matter laminations, and clay-tuffaceous laminations.

(2) Most of the BPFs in tight oil sandstones are unfilled, accounting for over 95%, with a few partially filled with calcite and bitumen, and few fully filled. The aperture of the fractures is generally less than 40 μm, primarily less than 10 μm, accounting for over 80%. The filling degree of the fractures varies with different apertures, with larger apertures having lower fill proportions. The P10 of fractures in argillaceous siltstone can reach up to 6 $cm^{-1}$, significantly higher than the fracture density in other lithologies (P10 ranging from 2.7–3.2 $cm^{-1}$).

(3) Bedding-parallel fractures exhibit a priority sequence in different types of laminations: increasing from sand, clay, organic matter to biotite and tuffaceous lamination, which reflects decreasing mechanical strength. However, the development degree of BPFs also depends on the mechanical contrast with their adjacent laminations. The greater the difference in mechanical

properties between adjacent laminations, the easier it is to fracture along the weak plane, and more intensive the bedding-parallel fractures development. Laminations density influences the density of related bedding-parallel fractures, with the $P_{10}$ of BPFs showing a pattern of increase followed by a decrease as lamination density increases. When the density of the laminations is within a certain range, as the density of the laminations increases, the number of BPFs also increases; When the density of the laminations continues to increase beyond this range, the plastic laminations consume some strain energy through plastic deformation, leading to a decrease in the degree of fractures. Lamination thickness affects the density and aperture of BPFs, with an increase in lamination thickness leading to a decrease in fracture density and an increase in aperture. BPFs in thick laminations mainly distribute along the edges of the laminations, while in thin laminations, the fractures mainly occur inside the laminations.

(4) When multiple types of laminations coexist, there is a competition between the influence of lamination type and lamination thickness on BPFs. Plastic thin laminations are conducive to the development of BPFs, while brittle thick laminations are not conducive to the formation of BPFs. When the thickness of the plastic laminations is close to or less than that of the brittle laminations, the laminations type has a dominant influence on BPFs, and the fractures tend to develop along the plastic laminations. When the thickness ratio of plastic laminations to brittle laminations is greater than 4, the influence of lamination thickness will dominate, and bedding-parallel fractures will tend to develop along the thin laminations.

## Data availability statement

The datasets presented in this study can be found in online repositories. The names of the repository/repositories and accession number(s) can be found in the article/Supplementary Material.

## Author contributions

HL: Conceptualization, Data curation, Investigation, Methodology, Writing–original draft, Writing–review and editing. SC: Conceptualization, Data curation, Methodology, Supervision, Writing–review and editing. SD: Data curation, Methodology, Writing–review and editing. WL: Writing–review and editing. LZ: Funding acquisition, Investigation, Project administration, Writing–review and editing.

## Funding

The author(s) declare that financial support was received for the research, authorship, and/or publication of this article. This work was financially supported by the National Natural Science Foundation of China (No. 42002135) and the Strategic Cooperation Technology Projects of CNPC and CUPB (No. ZLZX 2020–02).

## Conflict of interest

The authors declare that the research was conducted in the absence of any commercial or financial relationships that could be construed as a potential conflict of interest.

## Publisher's note



## References

Abaab, N., Zanella, A., Akrout, D., Mourgues, R., and Montacer, M. (2021). Timing and Distribution of Bedding-Parallel Veins, in Evaporitic Rocks, Bouhedma Formation, Northern Chotts, Tunisia. *J. Struct. Geol.* 153, 104461. doi:10.1016/j.jsg.sri2021.104461

Anders, M. H., Laubach, S. E., and Scholz, C. H. (2014). Microfractures: A Review. *J. Struct. Geol.* 69, 377–394. doi:10.1016/j.jsg.2014.05.011

Chen, A. Q., Chen, H. D., Hou, M. C., Lou, Z. H., Xu, S. L., Li, J., et al. (2011). The Middle-Late Triassic Event Sediments in Ordos Basin: Indicators for Episode I of Indosinian Movement. *Acta Geol. Sin.* 85 (10), 1681–1690. 11-1951/P.20110923.1427.002.

Cheng, S., Sheng, M., and Deng, C. (2024). Identification of Different lithofacies Laminations in Oil Shale and their Mechanical Properties. *Front. ENERGY Res.* 11. doi:10.3389/fenrg.2023.1321853

Cobbold, P. R., Zanella, A., Rodrigues, N., and Løseth, H. (2013). Bedding-Parallel Fibrous Veins (Beef and Cone-In-Cone): Worldwide Occurrence and Possible Significance in Terms of Fluid Overpressure, Hydrocarbon Generation and Mineralization. *Mar. Petroleum Geol.* 43, 1–20. doi:10.1016/j.marpetgeo.2013.01.010

Deng, X. Q., Lin, F. X., Liu, X. Y., Pang, J. L., Lyu, J. W., Li, S. X., et al. (2008). Discussion on relationship between sedimentary evolution of the Triassic Yanchang Formation and the Early Indosinian Movement in Ordos Basin. *J. Palaeogeo.* 10 (2), 159–166.

Dean, J. M., Kemp, A. E. S., and Pearce, R. B. (2001). Palaeo-Flux Records from Electron Microscope Studies of Holocene Laminated Sediments, Saanich Inlet, British Columbia. *Mar. Geol.* 174 (1), 139–158. doi:10.1016/S0025-3227(00)00147-X

Dong, S., Zeng, L., Wang, L., Du, X., Bao, M., Lyu, W., et al. (2022). An Intelligent Prediction Method of Fractures in Tight Carbonate Reservoirs. *Petroleum Explor. Dev.* 49 (6), 1364–1376. doi:10.1016/S1876-3804(23)60355-6

Dong, S., Zeng, L., Wang, L., Lyu, W., Xu, C., Liu, J., et al. (2020). Fracture Identification by Semi-Supervised Learning Using Conventional Logs in Tight Sandstones of Ordos Basin, China. *J. Nat. Gas Sci. Eng.* 76, 103131. doi:10.1016/j.jngse.2019.103131

Dong, S., Zeng, L., Wang, L., Lyu, W., Xu, H., Ji, C., et al. (2024). Fracture Identification In Shale Reservoir Using a Deep Learning Method: Chang 7 Reservoirs, Triassic Yanchang Formation. *Geoenergy Sci. Eng.* 238, 212853. doi:10.1016/j.geoen.2024.212853

Dong, S., Zeng, L., Zhong, Z., Cui, X., Zeng, L., Yang, X., et al. (2023). A Deep Kernel Method for Lithofacies Identification Using Conventional Well Logs. *Petroleum Sci.* 20 (3), 1411–1428. doi:10.1016/j.petsci.2022.11.027

Farouk, S., Qteishat, A., Sen, S., Ahmad, F., El-Kahtany, K., Collier, R., et al. (2024). Characterization of the Gas-Bearing Tight Paleozoic Sandstone Reservoirs of the Risha Field, Jordan: Inferences on Reservoir Quality and Productivity. *Arabian J. Sci. Eng.*, 1–21. doi:10.1007/s13369-024-09000-x

Feng, Z. H., Liu, B., Shao, H. M., and Wang, C. (2020). The Diagenesis Evolution and Accumulating Performance of the Mud Shale in Qingshankou Formation In Gulong Area, Songliao Basin. *Petroleum Geol. Oilfield Dev. Daqing* 39 (03), 72–85. doi:10.19597/J.ISSN.1000-3754.202004057

Fraino, P. E., Furlong, C. M., and Pedersen, P. K. (2022). Quantifying Centimeter-to Microscale Heterogeneities in Sedimentary, Compositional, and Geomechanical Properties of Siltstone Deposits in the Lower Triassic Montney Formation, Northeastern British Columbia, Canada. *Northeast. B. C. Can. Lithosphere* 2022 (2022), 1232390. doi:10.2113/2022/1232390

Fu, J. H., Li, S. X., Niu, X. B., Deng, X. Q., and Zhou, X. P. (2020). Geological Characteristics and Exploration of Shale Oil in Chang 7 Member of Triassic Yanchang Formation, Ordos Basin, NW China. *Petroleum Explor. Dev.* 47 (05), 931–945. doi:10.1016/s1876-3804(20)60107-0

Gorniak, K. (2017). Insights into Marls from Optical and Back-scattered Electron Petrography: An Example from the Outer Carpathians(Poland). *J. Sediment. Res.* 87 (3), 288–311. doi:10.2110/jsr.2017.16

Gou, Q. Y., and Xu, S. (2023). The Controls of Laminae on Lacustrine Shale Oil Contentin China: A Review from Generation, Retention, and Storage. *Energies* 16 (4), 1987. doi:10.3390/en16041987

Ju, W., You, Y., Feng, S. B., Xu, H. R., Zhang, X. L., and Wang, S. Y. (2020). Characteristics and Genesis of BPFs in Tight Sandstone Reservoirs of Chang 7 Oil Layer, Ordos Basin. *Oil Gas Geol.* 41 (03), 596–605. doi:10.11743/ogg20200315

Laubach, S., and Diaz-Tushman, K. (2009). Laurentian Palaeostress Trajectories and Ephemeral Fracture Permeability, Cambrian Eriboll Formation Sandstones West of the Moine Thrust Zone, NW Scotland. *J. Geol. Soc.* 166 (2), 349–362. doi:10.1144/0016-76492008-061

Lazar, O. R., Bohacs, K. M., Macquaker, J. H. S., Schieber, J., and Demko, T. M. (2015). Capturing Key Attributes of Fine-Grained Sedimentary Rocks In Outcrops, Cores, and Thin Sections: Nomenclature and Description Guidelines. *J. Sediment. Res.* 85 (3), 230–246. doi:10.2110/jsr.2015.11

Li, Q., Lu, H., Wu, S. H., Xia, D. L., Li, J. S., Qi, F. Q., et al. (2022). Sedimentary Origins and Reservoir Characteristics of the Triassic Chang 73 Tuffs in the Southern Ordos Basin. *Oil Gas Geol.* 43 (05), 1141–1154. doi:10.11743/ogg20220511

Luo, Q., Wei, H. Y., Liu, D. D., Zhang, C., Zhu, D. Y., Zhang, Y. Z., et al. (2017). Research Significance, Advances and Trends on the Role of Bedding Fracture in Tight Oil Accumulation. *Petroleum Geol. Exp.* 39 (01), 1–7. doi:10.11781/sysydz201701001

Nath, F., and Mokhtari, M. (2018). Optical Visualization of Strain Development and Fracture Propagation in Laminated Rocks. *J. Petroleum Sci. Eng.* 167, 354–365. doi:10.1016/j.petrol.2018.04.020

Ojala, A. E. K., and Tiljander, M. (2003). Testing the Fidelity of Sediment Chronology: Comparison of Varve and Paleomagnetic Results from Holocene Lake Sediments from Central Finland. *Quat. Sci. Rev.* 22 (15-17), 1787–1803. doi:10.1016/S0277-3791(03)00140-9

Pang, X., Wang, G., Kuang, L., Zhao, F., Li, C., Wang, C., et al. (2023). Lamellation Fractures in Shale Oil Reservoirs: Recognition, Prediction and their Influence on Oil Enrichment. *Mar. PETROLEUM Geol.* 148, 106032. doi:10.1016/j.marpetgeo.2022.106032

Sageman, B. B., Murphy, A. E., Werne, J. P., Straeten, C., Hollander, D. J., and Lyons, T. W. (2003). A Tale of Shales: The Relative Roles of Production, Decomposition, and Dilution in the Accumulation of Organic-Rich Strata, Middle-Upper Devonian, Appalachian Basin. *Chem. Geol.* 195 (1-4), 229–273. doi:10.1016/S0009-2541(02)00397-2

Sarhan, M. A., Ali, A. S., and Abdel-Fattah, M. I. (2023). Geophysical Assessment of Basement Rocks for Use as an Unconventional Reservoir in the Rabeh East Oil Field, Southern Gulf of Suez Basin. *Euro-Mediterranean J. Environ. Integration* 8 (2), 409–423. doi:10.1007/s41207-023-00372-4

Sarhan, M. A., Basal, A. M. K., and Ibrahim, I. M. (2017). Integration of Seismic Interpretation and Well Logging Analysis of Abu Roash D Member, Gindi Basin, Egypt: Implication For Detecting and Evaluating Fractured Carbonate Reservoirs. *J. Afr. Earth Sci.* 135, 1–13. doi:10.1016/j.jafrearsci.2017.08.010

Sarhan, M. A., and Selim, E. S. (2023). Geophysical Appraisal of Fractured Carbonate Reservoirs: A Case Study of Abu Roash D Member, Abu Gharadig Field, Western Desert, Egypt. *Euro-Mediterranean J. Environ. Integration* 8 (2), 395–408. doi:10.1007/s41207-023-00365-3

Schieber, J. (2011). Reverse Engineering Mother Nature - Shale Sedimentology from An Experimental Perspective. *Sediment. Geol.* 238 (1), 1–22. doi:10.1016/j.sedgeo.2011.04.002

Swanson, S. K. (2007). Lithostratigraphic Controls on Bedding-Plane Fractures and the Potential for Discrete Groundwater Flow through a Siliciclastic Sandstone Aquifer, Southern Wisconsin. *Sediment. Geol.* 197 (1-2), 65–78. doi:10.1016/j.sedgeo.2006.09.002

Xu, X., Zeng, L. B., Tian, H., Ling, K. G., Che, S. Q., Yu, X., et al. (2021). Controlling Factors of Lamellation Fractures in Marine Shales: A Case Study of the Fuling Area in Eastern Sichuan Basin, China. *J. Petroleum Sci. Eng.* 207, 109091. doi:10.1016/j.petrol.2021.109091

Yang, H., Li, S. X., and Liu, X. Y. (2013). Characteristics and Resource Prospects of Tight Oil and Shale Oil in Ordos Basin. *Acta Pet. Sin.* 34 (01), 1–11. doi:10.7623/syxb201301001

Zeng, L., Xu, X., Ma, S., Bao, H., Tian, H., Mao, Z., et al. (2024). Contribution of Lamellation Fractures to Porosity and Permeability of Shales: A Case Study of the Jiaoshiba Area in the Sichuan Basin, China. *GEOENERGY Sci. Eng.* 232 (A), 212439. doi:10.1016/j.geoen.2023.212439

Zeng, L. B., and Li, X. Y. (2009). Fractures in Sandstone Reservoirs with Ultra-Low Permeability: A Case Study of the Upper Triassic Yanchang Formation in the Ordos Basin, China. *AAPG Bull.* 93 (4), 461–477. doi:10.1306/sri09240808047

Zeng, L. B., Lyu, W., Xu, X., and Tian, H. (2022). Development Characteristics, Formation Mechanism and Hydrocarbon Significance of Bedding Fractures in Typical Tight Sandstone and Shale. *Acta Pet. Sin.* 43 (02), 180–191.sri doi:10.7623/syxb202202002

Zeng, L. B., Lyu, W. Y., Zhang, Y. Z., Liu, G. P., and Dong, S. Q. (2021a). The Effect of Multi-Scale Faults and Fractures on Oil Enrichment and Production in Tight Sandstone Reservoirs: A Case Study in the Southwestern Ordos Basin, China. *Front. Earth Sci.* 9. doi:10.3389/feart.2021.664629

Zeng, L. B., Lyu, W. Y., Zhu, L. F., Weng, J. Q., Yue, F., Zu, K. W., et al. (2016). Natural Fractures and their Influence on Shale Gas Enrichment in Sichuan Basin, China. *J. Nat. Gas Sci. Eng.* 30, 1–9. doi:10.1016/j.jngse.sri2015.11.048

Zeng, L. B., Shu, Z. G., Lyu, W. Y., Zhang, M. J., Bao, H. Y., Dong, S. Q., et al. (2021b). Lamellation Fractures in the Paleogene Continental Shale Oil Reservoirs in the Qianjiang Depression, Jianghan Basin, China. *Geofluid* 2021, 1–10. doi:10.1155/2021/6653299

Zhao, K., Du, X. B., Lu, Y. C., Xiong, S. P., and Wang, Y. (2019). Are Light-Dark Coupled Laminae in Lacustrine Shale Seasonally Controlled? A Case Study Using Astronomical Tuning From 42.2 to 45.4 Ma in the Dongying Depression, Bohai Bay Basin, Eastern China. *Palaeogeogr. Palaeoclimatol. Palaeoecol.* 528 (35), 35–49. doi:10.1016/j.palaeo.2019.04.034

Zhao, P. F., Wang, X. X., Fan, X. Y., Wang, X. Z., Zeng, F. T., Zhang, M. M., et al. (2021). The Influence of Lamina Density and Occurrence on the Permeability of Lamellar Shale after Hydration. *Crystals* 11 (12), 1524. doi:10.3390/sricryst11121524

Zou, C. N., Tao, S. Z., Yang, Z., Yuan, X. J., Zhu, R. K., Hou, L. H., et al. (2012). New advance in unconventional petroleum exploration and research in China. *Bull. Mine. Petr. Geochem.* 31 (4), 312–322. doi:10.3969/j.issn.1007-2802.2012.04.002